Numerical integration of an erythropoiesis model with explicit growth factor dynamics

O. Angulo, Fabien Crauste, J.C. López-Marcos

Numerical integration of an erythropoiesis model with explicit growth factor dynamics

O. Angulo[a,*], F. Crauste[b,c], J.C. López-Marcos[d]

[a] *Departamento de Matemática Aplicada. ETSIT. Universidad de Valladolid. Pso. Belén 5, 47011 Valladolid. SPAIN. Phone: +34 983 423000(Ext: 5835). FAX: +34 983 423661.*
[b] *Univ. Lyon, Université Lyon 1, CNRS UMR 5208, Institut Camille Jordan, 43 blvd du 11 novembre 1918, F-69622 Villeurbanne-Cedex, France*
[c] *Inria, Villeurbanne, France*
[d] *Departamento de Matemática Aplicada. Facultad de Ciencias. Universidad de Valladolid. Pso. Belén 7, 47011 Valladolid. SPAIN.*

Abstract

Erythropoiesis, the red blood cell production process, involves interactions between cell populations with different differentiation states, mainly immature progenitor cells and mature erythrocytes, and growth factors such as erythropoietin and glucocorticoids, known to respectively inhibit cell apoptosis, stimulate proliferation and differentiation, and stimulate self-renewal. The feedback regulation of this process allows a very fast and efficient recovery in the case of a severe anemia. We consider an age-structured model of red blood cell production accounting for these feedback regulations and the dynamics of growth factors. We theoretically show the existence of a unique positive steady state for the model and we propose a numerical method to obtain an approximation to its solution. Experiments are reported to show numerically, on one hand, the optimal convergence order of the numerical scheme and, on the other hand, a fine approximation to real experimental data, with a suitable selection of the parameters involved.

Keywords: erythropoiesis model, nonlinear age-structured system, numerical scheme, long-time integration
2000 MSC: 65M25, 35B40, 35L60, 35Q92, 92D25

1. Introduction

Production of red blood cells occurs in the bone marrow, where undifferentiated immature hematopoietic stem cells differentiate, throughout a number of divisions, into more and more mature cells until fully differentiated mature red blood cells are produced. The process of production and regulation of red blood cells is called erythropoiesis. The first stage of differentiation of hematopoietic stem cells is the progenitor stage: erythroid progenitors are undifferentiated cells committed to the red blood cell – or erythroid – lineage. These cells share

*Corresponding author
Email addresses: oscar@mat.uva.es (O. Angulo), crauste@math.univ-lyon1.fr (F. Crauste), lopezmar@mac.uva.es (J.C. López-Marcos)

a lot of properties with stem cells, such as the ability to proliferate and differentiate but also to self-renew, that is to produce by division two daughter cells identical to the mother cell. Erythroid progenitors proliferate and differentiate in more mature cells, meanwhile losing their self-renewal ability, until they reach the stage of reticulocytes. These latter are immature red blood cells that will finish their differentiation process within few divisions, ejecting their nucleus, and finally differentiating in erythrocytes that leave the bone marrow and enter the bloodstream as red blood cells. The entire process is regulated by a variety of feedback controls, involving growth factors. Among them, erythropoietin has been identified in 1990 as the main regulator of erythropoiesis: released by the kidneys when the organism detects a lack of red blood cells, erythropoietin binds to the surface of erythroid progenitors and prevents their death, called apoptosis, hence increasing the amount of differentiated cells [24]. Glucocorticoids have also been shown to influence erythropoiesis in stress conditions by inducing erythroid progenitor self-renewal [15, 22].

We propose a mathematical model of stress erythropoiesis in mice based on age-structured nonlinear partial differential equations describing erythroid progenitor and erythrocyte dynamics in the next section. This model is based on previous models, proposed in [8, 21], that were inspired by the initial works by Mackey [26] and co-authors, and Loeffler et al. [25, 33], to describe stress erythropoiesis in mice. Several mathematical models of erythropoiesis have been proposed over the last 30 years (see [32] for a review), in order to address the mechanisms of regulation and their role in stress or pathological conditions. Mackey Mackey [26] published a pioneering paper on hematopoietic stem cell dynamics, which has then been used and modified by many authors, including Mackey and co-workers, to describe differentiation and maturation processes involved in hematopoiesis more precisely [4, 5, 18, 19, 31]. Belair et al [16] proposed a model of erythropoiesis considering the influence of growth factors on stem cell differentiation in erythroid progenitors, later improved by Mahaffy et al [27], and recently analyzed in more details [2, 3]. Another erythropoiesis model, inspired by the same article, was introduced by Adimy et al. [6] in 2006, in which Epo is the only growth factor supposed to act during erythropoiesis. An important contribution to mathematical modeling of erythropoiesis is also due to Loeffler and his collaborators [25, 32, 37]. Their models consider feedback controls from progenitors on the stem cell level and from mature cells on progenitors, and were fitted to various experiments (including irradiations, bleeding, and phenylhydrazine treatments of mice). Most of these works were nevertheless performed before the role of Epo was definitely identified and long before erythroid progenitor self-renewal was hypothesized.

The equations we propose are coupled via age-dependent feedback functions associated with cell ability to die by apoptosis, to self-renew and to differentiate. Contrary to previous, simpler models on which it is based [8, 21], that partially described regulation of erythropoiesis (for instance, none of them described age-dependency of feedback functions, and only the model studied in [8] assumed a non-constant mortality rate of erythrocytes), our model additionally considers explicit growth factor dynamics, unlike all previously published models of erythropoiesis (except for Adimy et al. [6]). We first establish the theoretical existence of a unique positive stationary solution in section 3 then propose a new numerical scheme to simulate solutions of the system in section 4. In section 5 we illustrate the efficiency of our method by showing numerically that it is of

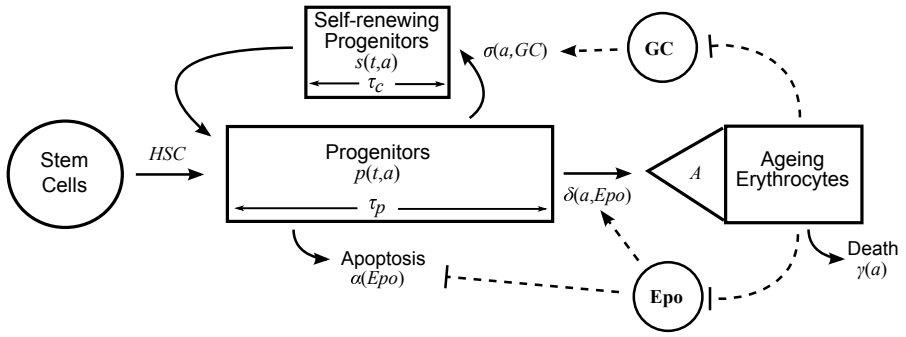

Figure 1: **Schematic Model of Erythropoiesis.** Plain lines with arrows represent cell process (differentiation, death, proliferation, cell cycle), whereas dashed lines represent feedback controls.

second order of convergence, and that it allows to compare simulated solutions of the model with real biological data.

2. Model of Stress Erythropoiesis

Let consider a population of erythroid progenitors and a population of erythrocytes, defined by cell age a and the time of the observation t (see Figure 1). Cell age a is considered to be the time spent from the birth of a cell up to the time of observation, hence cells age with unitary velocity (see (4)). Among progenitors, a difference is made between self-renewing progenitors, whose population is denoted by $s(t,a)$, and differentiating progenitors that are not self-renewing, denoted by $p(t,a)$. The duration of the differentiating progenitor compartment is denoted by τ_p, and the duration of one self-renewing cycle by τ_c. One may note that $\tau_c < \tau_p$. All progenitors are supposed to be localized in the bone marrow, and all of them can die by apoptosis. The number of erythrocytes, circulating in blood, is denoted by $e(t,a)$, and $E(t)$ denotes the total number of erythrocytes at time t, defined by

$$E(t) = \int_0^{+\infty} e(t,a)da.$$

Two growth factors, erythropoietin (Epo) and glucocorticoids (GC), are assumed to be the main regulators of erythroid progenitor apoptosis and differentiation, and self-renewal respectively [21]. Denote by $Epo(t)$ the concentration of Epo at time t in bloodstream, and by $GC(t)$ the concentration of glucocorticoids at time t. These concentrations are regulated by the total number of erythrocytes $E(t)$: the more erythrocytes, the less Epo and glucocorticoids [15, 24].

Denote by $\alpha(Epo)$ the erythroid progenitor apoptosis rate, and by $\sigma(a, GC)$ the erythroid progenitor self-renewal rate. The function α is assumed to be decreasing with respect to Epo (negative feedback, [24]). The function σ is assumed to be increasing with respect to GC (positive feedback), and decreasing with respect to the age a of progenitor cells [15] with $\sigma(\tau_p, GC) = 0$. This latter assumption illustrates a lack of sensitivity to GC of mature progenitors,

contrary to early progenitors that are more sensitive to GC. These assumptions are summarized hereafter, with ∂_x denoting the partial derivative with respect to x:

$$\alpha'(Epo) \leq 0, \quad \partial_a \sigma(a, GC) \leq 0, \quad \partial_{GC}\sigma(a, GC) \geq 0, \quad \sigma(\tau_p, GC) = 0.$$

Denote by $\delta(a, Epo)$ the differentiation rate of progenitors into erythrocytes. This rate depends on the age of progenitors, older ones being more inclined to differentiate [23], and on the concentration of Epo, the more Epo the more differentiation [23]. The function δ is hence assumed to be increasing with respect to a and Epo,

$$\partial_a \delta(a, Epo) > 0, \qquad \partial_{Epo}\delta(a, Epo) > 0.$$

In addition, since all progenitors which did not die in the differentiating compartment must differentiate in erythrocytes, we assume $\lim_{a\to\tau_p} \delta(a, Epo) = +\infty$ whatever the level of Epo.

The following functions α, σ and δ, will be used in section 5 to perform numerical experiments,

$$\alpha(Epo) = C_\alpha \frac{\theta_\alpha^{n_\alpha}}{\theta_\alpha^{n_\alpha} + (\log_{10}(Epo))^{n_\alpha}}, \tag{1}$$

where $C_\alpha > 0$ is the maximal apoptosis rate, $\theta_\alpha > 0$ is a threshold value, and $n_\alpha > 1$ is a sensitivity parameter;

$$\sigma(a, GC) = C_\sigma(\tau_p - a)\frac{(\log_{10}(GC))^{n_\sigma}}{\theta_\sigma^{n_\sigma} + (\log_{10}(GC))^{n_\sigma}}, \tag{2}$$

where, similarly to the function α, $\theta_\sigma > 0$, $n_\sigma > 1$, and $C_\sigma > 0$ is a constant characterizing the maximum self-renewal rate given, for a fixed value of GC, by $C_\sigma(\tau_p - a)$;

$$\delta(a, Epo) = C_{\delta_1}\frac{\tau_p}{\tau_p - a} + C_{\delta_2}\frac{(\log_{10}(Epo))^{n_\delta}}{\theta_\delta^{n_\delta} + (\log_{10}(Epo))^{n_\delta}} =: \delta_1(a) + \delta_2(Epo), \tag{3}$$

where C_{δ_1} is the minimum of the age-dependent differentiation rate $\delta_1(a)$, reached when $a = 0$, C_{δ_2} is the maximum of the Epo-dependent differentiation rate $\delta_2(Epo)$, and $C_{\delta_1} > 0$, $C_{\delta_2} > 0$, $\theta_\delta > 0$ is a threshold value for the Epo-dependent part of the differentiation rate, $n_\delta > 1$ a sensitivity parameter.

It must be noted that in the absence of GC, the self-renewal rate is supposed to vanish, whatever the age of cells, whereas differentiation occurs in the presence or the absence of Epo: Epo is assumed to positively act on erythroid progenitor differentiation, yet differentiation can be induced independently of Epo levels. This explains why the differentiation rate is composed of two additive terms, whereas the self-renewal rate is composed of only one term.

Denote by γ the mortality rate of erythrocytes. To our knowledge, no precise measurement of this rate is available in the literature, so it is usually supposed to be constant. It can however be modified under specific circumstances (see [21] and section 5 for instance), so without loss of generality we will consider that it depends on both erythrocyte age a and observation time t, and we will write $\gamma(t, a)$ (see [8]).

Then, the quantities p, s and e satisfy the following system, for $t > 0$,

$$\begin{cases} \partial_t p(t,a) + \partial_a p(t,a) = -\left[\alpha(Epo(t)) + \delta(a, Epo(t))\right] p(t,a) \\ \qquad\qquad -\sigma(a, GC(t)) p(t,a), & a \in (0, \tau_p), \\ \partial_t s(t,a) + \partial_a s(t,a) = -\alpha(Epo(t)) s(t,a), & a \in (0, \tau_c), \\ \partial_t e(t,a) + \partial_a e(t,a) = -\gamma(t,a) e(t,a), & a > 0. \end{cases} \tag{4}$$

Boundary conditions associated with (4) describe cell flux between compartments,

$$\begin{cases} p(t,0) &= HSC + 2s(t,\tau_c), \\ s(t,0) &= \displaystyle\int_0^{\tau_p} \sigma(a, GC(t)) p(t,a) da, \\ e(t,0) &= A \displaystyle\int_0^{\tau_p} \delta(a, Epo(t)) p(t,a) da. \end{cases} \tag{5}$$

New erythroid progenitors come both from the division of self-renewing progenitors in two newborn cells and the differentiation of hematopoietic stem cells: HSC denotes the flux of hematopoietic stem cells differentiating in erythroid progenitors, assumed to be constant over time. Self-renewing progenitors are produced at a rate σ from differentiating progenitors. Erythrocytes are produced from differentiating progenitors, and A denotes a constant amplification coefficient accounting for divisions of mature progenitors. For instance, $A = 2^n$ where n is the number of differentiation stages during the reticulocyte stage [21].

Concentrations of growth factors $Epo(t)$ and $GC(t)$ satisfy the following ordinary differential equations [20],

$$\begin{cases} \dfrac{d}{dt} Epo(t) &= f(E(t)) - k_{Epo} Epo(t), \\ \dfrac{d}{dt} GC(t) &= g(E(t)) - k_{GC} GC(t), \end{cases} \tag{6}$$

where $k_{Epo} > 0$ and $k_{GC} > 0$ are degradation rates, and the functions f and g describe feedback controls by the total number of erythrocytes on the production of growth factors. Both functions are assumed to be decreasing (see Figure 1),

$$f'(E) < 0, \qquad g'(E) < 0.$$

The model is completed with suitable initial conditions

$$\begin{cases} p(0,a) &= p_0(a), \quad a \in [0, \tau_p], \\ s(0,a) &= s_0(a), \quad a \in [0, \tau_c], \\ e(0,a) &= e_0(a), \quad a > 0, \\ Epo(0) &= Epo_0, \\ GC(0) &= GC_0. \end{cases} \tag{7}$$

Existence and uniqueness of solutions of system (4)–(7) follow from the classical theory of age-structured equations [36], under conditions of smoothness of the various nonlinear feedback functions. In section 3, we analyze the existence of stationary solutions for this model.

The effort made on increasing the realism in the model is however achieved at the expense of loss in mathematical tractability. We point out that, without other restrictive assumptions, this model cannot be solved analytically. Therefore, the use of efficient methods that provide a numerical approach is the most suitable mathematical tool for studying the problem and, indeed, it is often the only one available. Besides, numerical methods have been successfully applied to structured models to replicate available field and/or laboratory data for a variety of different systems (e.g. [9, 11, 12, 13] and references therein). We completely describe, in section 4, the explicit second order numerical scheme, built "ad hoc", which has been used to obtain the solutions of (4)–(7). And, finally, we perform a wide numerical experimentation which includes convergence, long-time integration with the simulation of the theoretical steady state and a comparison with real biological data in section 5.

3. Existence of a Positive Steady State

We focus in this section on the existence of steady states for system (4)–(6) when γ does not depend on time t, that is in normal erythropoiesis. From a biological point of view, system (4)–(6) is expected to possess in this case only one positive steady state, due to the constant positive flux HSC from the hematopoietic stem cell compartment.

Suppose $(p^*(a), s^*(a), e^*(a), Epo^*, GC^*)$ is a steady state solution of system (4)–(6). Then, it satisfies

$$\begin{cases} \dfrac{dp^*}{da}(a) = -\left[\alpha(Epo^*) + \sigma(a, GC^*) + \delta(a, Epo^*)\right] p^*(a), & a \in (0, \tau_p), \\ \dfrac{ds^*}{da}(a) = -\alpha(Epo^*) s^*(a), & a \in (0, \tau_c), \\ \dfrac{de^*}{da}(a) = -\gamma(a) e^*(a), & a > 0, \end{cases} \tag{8}$$

with

$$\begin{cases} p^*(0) &= HSC + 2s^*(\tau_c), \\ s^*(0) &= \displaystyle\int_0^{\tau_p} \sigma(a, GC^*) p^*(a) da, \\ e^*(0) &= A \displaystyle\int_0^{\tau_p} \delta(a, Epo^*) p^*(a) da, \end{cases} \tag{9}$$

and

$$k_{Epo} Epo^* = f(E^*), \qquad k_{GC} GC^* = g(E^*),$$

where

$$E^* = \int_0^{+\infty} e^*(a) da. \tag{10}$$

Let us introduce the following notations,

$$\begin{cases} \bar{\alpha}(E^*) &:= \alpha(F(E^*)), & \\ \bar{\sigma}(a, E^*) &:= \sigma(a, G(E^*)), & a \in [0, \tau_p], \\ \bar{\delta}(a, E^*) &:= \delta(a, F(E^*)), & a \in [0, \tau_p], \\ \beta(a, E^*) &:= \bar{\alpha}(E^*) + \bar{\sigma}(a, E^*) + \bar{\delta}(a, E^*), & a \in [0, \tau_p], \end{cases}$$

where $F(E^*) := f(E^*)/k_{Epo}$ and $G(E^*) := g(E^*)/k_{GC}$. Consider the following assumptions,

(H1) Suppose for all $\theta \in [0, \tau_p]$,

$$\partial_Y \beta(\theta, Y) > 0, \qquad \forall Y \geq 0.$$

(H2) Suppose, for all $\theta \in [0, \tau_p]$, there exists $\bar{Y} > 0$ such that

$$\begin{cases} \partial_Y \beta(\theta, Y) < 0, & \forall Y \in [0, \bar{Y}), \\ \partial_Y \beta(\theta, Y) > 0, & \forall Y \in (\bar{Y}, +\infty). \end{cases}$$

From a biological point of view, Assumption (H1) describes a situation in which as the number of erythrocytes increases progenitor apoptosis increases. This is expected, otherwise the erythrocyte population could be unbounded. Assumption (H2) has a similar interpretation, but it also considers that for small erythrocytes counts, progenitor apoptosis rate becomes negligible compared to self-renewal and differentiation rates. This should theoretically allow a repopulation of the erythrocyte population. Both assumptions are in agreement with biological knowledge.

The next proposition states the existence of a unique positive steady state.

Proposition 1. *Assume inequality*

$$e^{-\alpha(0)\tau_c} \int_0^{\tau_p} \sigma(a,0) \exp\left(- \int_0^a \alpha(0) + \sigma(\theta,0) + \delta(\theta,0) d\theta \right) da < \frac{1}{2} \tag{11}$$

holds true. Then whether Assumption (H1) or (H2) is satisfied, system (4)–(6) has a unique steady state.

Proof. This proof is in two parts. We first show that system (8)–(10) has a solution if and only if condition (21) holds true. Then, as a second step, we show that under Assumption (H1) or (H2) condition (21) holds true as soon as (11) is satisfied.

Step 1. Solving system (8)–(9) gives

$$p^*(a) = \exp\left(- \int_0^a \beta(\theta, E^*) d\theta \right) [HSC + 2s^*(\tau_c)], \qquad a \in [0, \tau_p], \tag{12}$$

$$s^*(a) = \exp\left(-\bar{\alpha}(E^*)a\right) \int_0^{\tau_p} \bar{\sigma}(\theta, E^*) p^*(\theta) d\theta, \qquad a \in [0, \tau_c], \tag{13}$$

$$e^*(a) = \exp\left(- \int_0^a \gamma(\theta) d\theta \right) A \int_0^{\tau_p} \bar{\delta}(\theta, E^*) p^*(\theta) d\theta, \qquad a > 0. \tag{14}$$

Using (13) in (12), we deduce

$$p^*(a) = \exp\left(- \int_0^a \beta(\theta, E^*) d\theta \right) \Psi(E^*, p^*), \quad a \in [0, \tau_p], \tag{15}$$

where

$$\Psi(E^*, p^*) := HSC + 2e^{-\bar{\alpha}(E^*)\tau_c} \int_0^{\tau_p} \bar{\sigma}(\theta, E^*) p^*(\theta) d\theta. \tag{16}$$

Using now (15) in (14) one obtains

$$e^*(a) = \exp\left(-\int_0^a \gamma(\theta)d\theta\right) A\Lambda(E^*)\Psi(E^*,p^*), \quad a>0,$$

with

$$\Lambda(E^*) := \int_0^{\tau_p} \bar{\delta}(\theta,E^*)\exp\left(-\int_0^\theta \beta(u,E^*)du\right)d\theta. \tag{17}$$

It follows that

$$E^* := \int_0^{+\infty} e^*(a)da = \xi A\Lambda(E^*)\Psi(E^*,p^*), \tag{18}$$

where

$$\xi := \int_0^{+\infty} \exp\left(-\int_0^a \gamma(\theta)d\theta\right)da > 0.$$

From (15), one gets for $a\in[0,\tau_p]$

$$\bar{\sigma}(a,E^*)p^*(a) = \bar{\sigma}(a,E^*)\exp\left(-\int_0^a \beta(\theta,E^*)d\theta\right)\Psi(E^*,p^*). \tag{19}$$

Introducing the following notations,

$$\left\{\begin{array}{lcl} \mu(E^*) & := & e^{-\bar{\alpha}(E^*)\tau_c}, \\ \nu(E^*) & := & \displaystyle\int_0^{\tau_p} \bar{\sigma}(a,E^*)\exp\left(-\int_0^a \beta(\theta,E^*)d\theta\right)da, \end{array}\right. \tag{20}$$

and using (16), we finally get from the integration of (19)

$$[1-2\mu(E^*)\nu(E^*)]\int_0^{\tau_p}\bar{\sigma}(\theta,E^*)p^*(\theta)d\theta = \nu(E^*)HSC.$$

Hence, providing that $1-2\mu(E^*)\nu(E^*)\neq 0$, we have from (16)

$$\Psi(E^*,p^*) = HSC + 2\mu(E^*)\frac{\nu(E^*)HSC}{1-2\mu(E^*)\nu(E^*)} = \frac{HSC}{1-2\mu(E^*)\nu(E^*)},$$

and from (18)

$$\Psi(E^*,p^*) = \frac{E^*}{A\xi\Lambda(E^*)}.$$

This yields that system (4)–(6) has a steady state $(p^*(a), s^*(a), e^*(a), Epo^*, GC^*)$, with $\int_0^{+\infty} e^*(a)da := E^*$, if

$$1-2\mu(E^*)\nu(E^*)\neq 0 \quad \text{and} \quad E^* = A.HSC.\xi\frac{\Lambda(E^*)}{1-2\mu(E^*)\nu(E^*)}. \tag{21}$$

Conversely, suppose there exists a constant $X>0$ such that

$$1-2\mu(X)\nu(X)\neq 0 \quad \text{and} \quad X = A.HSC.\xi\frac{\Lambda(X)}{1-2\mu(X)\nu(X)}.$$

Define

$$K := HSC\frac{\nu(X)}{1-2\mu(X)\nu(X)},$$

and set

$$\begin{cases} z(a) &= \exp\left(-\int_0^a \beta(\theta,X)d\theta\right)\left[HSC+2\mu(X)K\right], & a\in[0,\tau_p],\\ y(a) &= \exp\left(-\bar{\alpha}(X)a\right)K, & a\in[0,\tau_c],\\ x(a) &= \exp\left(-\int_0^a \gamma(\theta)d\theta\right)A.\Lambda(X)\left[HSC+2\mu(X)K\right], & a>0. \end{cases}$$

Then, it is straightforward, using (20) and setting $Epo^* = F(X)$ and $GC^* = G(X)$, to check that (z,y,x) satisfies (8)–(9) and (10). In particular, using the definition of x and ξ one obtains

$$\int_0^{+\infty} x(a)da = A\xi\Lambda(X)\left[HSC+2\mu(X)K\right],$$

and using the definitions of K and X one finally gets

$$\int_0^{+\infty} x(a)da = A.HSC.\xi\Lambda(X)\left[1+2\mu(X)\frac{\nu(X)}{1-2\mu(X)\nu(X)}\right] = X,$$

so (10) is satisfied. This defines a steady state solution of system (4)–(6).

Step 2. We now prove that, under assumptions (H1) or (H2), there exists a unique $E^* > 0$ satisfying (21). We first set

$$\chi(Y) := 1-2\mu(Y)\nu(Y), \qquad Y\geq 0,$$

and focus on the problem

$$\text{Find } Y\geq 0 \text{ such that } \chi(Y)>0 \text{ and } cY = \frac{\Lambda(Y)}{\chi(Y)}, \tag{22}$$

where $c := 1/(A.HSC.\xi) > 0$. From (17) and (20), and the previous assumptions on the functions α, σ and δ (see section 2), we obtain

$$\frac{d}{dY}\Lambda(Y) = \int_0^{\tau_p}\left[\partial_Y\bar{\delta}(\theta,Y) - \left(\int_0^\theta \partial_Y\beta(u,Y)du\right)\bar{\delta}(\theta,Y)\right]e^{-\int_0^\theta\beta(u,Y)du}d\theta,$$

and

$$\frac{d}{dY}\nu(Y) = \int_0^{\tau_p}\left[\partial_Y\bar{\sigma}(\theta,Y) - \left(\int_0^\theta \partial_Y\beta(u,Y)du\right)\bar{\sigma}(\theta,Y)\right]e^{-\int_0^\theta\beta(u,Y)du}d\theta,$$

and $\bar{\delta}(\theta,Y)>0$, $\bar{\sigma}(\theta,Y)>0$, $\partial_Y\bar{\delta}(\theta,Y)<0$ and $\partial_Y\bar{\sigma}(\theta,Y)<0$.

First assume (H1) holds true. Then

$$\frac{d}{dY}\Lambda(Y)<0 \quad \text{and} \quad \frac{d}{dY}\nu(Y)<0 \quad \text{for } Y\geq 0.$$

A first consequence, since by definition $d\mu(Y)/dY < 0$, is that

$$\frac{d}{dY}\chi(Y) = -2\left[\nu(Y)\frac{d}{dY}\mu(Y) + \mu(Y)\frac{d}{dY}\nu(Y)\right] > 0.$$

Hence, the function χ is increasing on $[0, +\infty)$. Moreover, (11) implies that $\lim_{Y\to+\infty}\chi(Y) > 0$. Hence, there exists $Y_0 \geq 0$ such that $\chi(Y) > 0$ for $Y \in (Y_0, +\infty)$ and $\chi(Y_0) \geq 0$.

Moreover, from (H1) and as long as $\chi(Y) > 0$,

$$\frac{d}{dY}\left(\frac{\Lambda(Y)}{\chi(Y)}\right) = \frac{\chi(Y)\frac{d}{dY}\Lambda(Y) - \Lambda(Y)\frac{d}{dY}\chi(Y)}{\chi(Y)^2} < 0.$$

Hence, the function $\Lambda(Y)/\chi(Y)$ is decreasing on the domain $(Y_0, +\infty)$, and $\Lambda(Y_0)/\chi(Y_0) > 0$. Consequently (22) has a unique solution $Y > Y_0$.

Assume (H2) holds true. Similarly to the above reasoning, $\Lambda(Y)$ and $\nu(Y)$ are decreasing on $(\bar{Y}, +\infty)$, and the function $\Lambda(Y)/\chi(Y)$ is decreasing for $Y > \max\{Y_0, \bar{Y}\}$. We then conclude similarly to the previous case to the existence and uniqueness of $Y > \max\{Y_0, \bar{Y}\}$ satisfying (22).

Under assumptions (H1) or (H2) we can then define a unique steady state to our problem. This concludes the proof. □

Let us briefly comment on (11). This condition implies that no more than half of the progenitor population can self-renew in order to obtain a stationary solution. Indeed, the term $\exp\left(-\int_0^a \alpha(0) + \sigma(\theta, 0) + \delta(\theta, 0)d\theta\right)$ describes the survival rate of differentiating progenitors, $\sigma(a, 0)$ refers to the maximal fraction of the population that will self-renew, and $\exp(-\alpha(0)\tau_c)$ is the maximal survival fraction of self-renewing progenitors. Inequality (11) is satisfied with our choices for α, σ and δ (see Equations (1), (2), (3)). If inequality (11) is not satisfied, then one may hypothesize the non-existence of a stationary solution and the unboundedness of the cell population.

4. Numerical Scheme

We introduce a new numerical method to simulate the system (4)-(7). It is based on the integration along the characteristic curves with the use of a representation formula of the solution [1].

The existence of a maximum age of differentiation, τ_p, makes the differentiation rate δ unbounded. This fact has been circumvented in [7, 14] with the use of an exact integration value at the end of the age-differentiation interval. However, this method is only possible when such an exact value is known, and this only happens with specific functions. In general, it is necessary to introduce a new different dependent function as in [30]. We assume, from now on, that age and Epo dependences of the function δ are independent, and we write, as in (3), $\delta(a, Epo) = \delta_1(a) + \delta_2(Epo)$.

Thus, let $q(t, a)$ be defined as $p(t, a) = \Pi(a)\, q(t, a)$, where

$$\Pi(a) = \exp\left(-\int_0^a \delta_1(x)\, dx\right),$$

and, accordingly, $p_0(a) = \Pi(a)\, q_0(a)$. The first equation of (4) is replaced with

$$\partial_t\, q + \partial_a\, q = -(\alpha(Epo(t)) + \delta_2(Epo(t)) + \sigma(a, GC(t)))\, q, \quad a \in (0, \tau_p). \tag{23}$$

This change also modifies the boundary condition (5), that writes

$$\left\{\begin{array}{rcl} q(t,0) & = & HSC + 2s(t,\tau_c), \\ s(t,0) & = & \displaystyle\int_0^{\tau_p} \sigma(a, GC(t))\, \Pi(a)\, q(t,a) da, \\ e(t,0) & = & \displaystyle A\int_0^{\tau_p} \delta(a, Epo(t))\, \Pi(a)\, q(t,a) da. \end{array}\right. \tag{24}$$

The unbounded age domain for erythrocytes is another circumstance that must be avoided in the numerical integration. Thus, we introduce a maximum age $A_{\max}$ for erythrocytes as in [7], that would be large enough to simulate the dynamics of the model. This means that the numerical method approaches the evolution of a "truncated" version of problem (23)-(24) and (6)-(7), which in turn is an approximation to the solution of the original problem (see [10]).

The formula we use in the numerical method is based on the theoretical integration along the characteristics, which gives us the next representation of the solution to the new system,

$$\left\{\begin{array}{l} q(t_* + h, a_* + h) \\ \quad = q(t_*, a_*)\, \exp\left(-\displaystyle\int_0^h \beta^*(a_* + x, Epo(t_* + x), GC(t_* + x))\, dx\right), \\ \quad a_* + h \le \tau_p, \\ s(t_* + h, a_* + h) \\ \quad = s(t_*, a_*)\, \exp\left(-\displaystyle\int_0^h \alpha(Epo(t_* + x))\, dx\right),\ a_* + h \le \tau_c, \\ e(t_* + h, a_* + h) \\ \quad = e(t_*, a_*)\, \exp\left(-\displaystyle\int_0^h \gamma(t_* + x)\, dx\right),\ a_* + h \le A_{\max}, \end{array}\right. \tag{25}$$

where $\beta^*(a, E, G) = \alpha(E) + \delta_2(E) + \sigma(a, G)$. Note that, in this new layout, we have two different problems: solving (25), which provides the solution to the population densities, and integrating (6), which gives the solution to the growth factor concentrations. We use discretization procedures in order to solve them.

We consider the numerical integration of model (23)-(24) and (6)-(7) along the time interval $[0, T]$. Thus, given a positive integer J_c, we define $h = \tau_c/J_c$, $J_p = [\tau_p/h]$, $J_{\max} = A_{\max}/h$ and $N = [T/h]$ (it is usual that τ_c and τ_p would be proportional, and $A_{\max}$ might be chosen to be proportional to τ_c, these restrictions do not play an important role in the numerical integration). We introduce the discrete time levels $t^n = n\, h$, $0 \le n \le N$, and the grid nodes $a_j = j\, h$, $0 \le j \le J_{\max}$. Then, we denote the numerical approximations to the theoretical solutions by: Q_j^n to $q_j^n = q(a_j, t_n)$, $0 \le j \le J_p$; S_j^n to $s_j^n = s(a_j, t_n)$, $0 \le j \le J_c$; I_j^n to $e_j^n = e(a_j, t_n)$, $0 \le j \le J_{\max}$; O^n to $o^n = Epo(t^n)$; and G^n to $g^n = GC(t^n)$; $0 \le n \le N$. We propose a new method to obtain them: (i) we start from an approximation of the initial data (7) of the problem, for instance

the grid restriction of functions q_0, s_0, e_0 and the values Epo_0 and GC_0, and (ii) the numerical solution at a new time level is described in terms of the previous one by means of a two steps scheme.

Such a general time level is obtained by means of the following second-order discretization of (24)-(25) and (6). For, $0 \leq n \leq N-1$,

$$\begin{array}{rl} Q_{j+1}^{n+1} = & Q_j^n \, \exp\left(-h\left(\beta^*(a_j, O^n, G^n) + \beta^*(a_{j+1}, O^{n+1,*}, G^{n+1,*})\right)/2\right), \\ & 0 \leq j \leq J_p - 1, \\ S_{j+1}^{n+1} = & S_j^n \, \exp\left(-h\left(\alpha(O^n) + \alpha(O^{n+1,*})\right)/2\right),\ 0 \leq j \leq J_c - 1, \\ I_{j+1}^{n+1} = & I_j^n \, \exp\left(-h\left(\gamma(a_j, t^n) + \gamma(a_{j+1}, t^{n+1})\right)/2\right),\ 0 \leq j \leq J_{\max} - 1, \end{array}$$

with

$$\begin{array}{rcl} Q_0^{n+1} & = & HSC + 2\, S_{J_c}^{n+1}, \\ S_0^{n+1} & = & \mathcal{Q}_h(\boldsymbol{\sigma}^{n+1} \cdot \boldsymbol{\Pi} \cdot \mathbf{Q}^{n+1}), \\ I_0^{n+1} & = & A\, \mathcal{Q}_h(\boldsymbol{\delta}^{n+1} \cdot \boldsymbol{\Pi} \cdot \mathbf{Q}^{n+1}), \end{array}$$

and

$$\begin{array}{rcl} O^{n+1} & = & O^n + h\left(f(\mathcal{Q}_h(\mathbf{I}^n)) + f(\mathcal{Q}_h(\mathbf{I}^{n+1,*})) - k_{Epo}\left(O^n + O^{n+1,*}\right)\right)/2, \\ G^{n+1} & = & G^n + h\left(g(\mathcal{Q}_h(\mathbf{I}^n)) + g(\mathcal{Q}_h(\mathbf{I}^{n+1,*})) - k_{GC}\left(G^n + G^{n+1,*}\right)\right)/2. \end{array}$$

Where the intermediate step is given by

$$\begin{array}{rcl} Q_{j+1}^{n+1,*} & = & Q_j^n \, \exp\left(-h\, \beta^*(a_j, O^n, G^n)\right),\ 0 \leq j \leq J_p - 1, \\ S_{j+1}^{n+1,*} & = & S_j^n \, \exp\left(-h\, \alpha(O^n)\right),\ 0 \leq j \leq J_c - 1, \\ I_{j+1}^{n+1,*} & = & I_j^n \, \exp\left(-h\, \gamma(a_j, t^n)\right),\ 0 \leq j \leq J_{\max} - 1, \end{array}$$

with

$$\begin{array}{rcl} Q_0^{n+1,*} & = & HSC + 2\, S_{J_c}^{n+1,*}, \\ I_0^{n+1,*} & = & A\, \mathcal{Q}_h(\boldsymbol{\delta}^{n+1,*} \cdot \boldsymbol{\Pi} \cdot \mathbf{Q}^{n+1,*}), \end{array}$$

and

$$\begin{array}{rcl} O^{n+1,*} & = & O^n + h\left(f(\mathcal{Q}_h(\mathbf{I}^n)) - k_{Epo}\, O^n\right), \\ G^{n+1,*} & = & G^n + h\left(g(\mathcal{Q}_h(\mathbf{I}^n)) - k_{GC}\, G^n\right). \end{array}$$

One can note that initializing $S_0^{n+1,*}$ is not necessary. In these formulae, $\mathcal{Q}_h(\mathbf{V}^n)$ represents a quadrature rule to approximate the integral on the interval $[0, A_{\max}]$ (approximation to the total number of erythrocytes $E(t)$) or $[0, \tau_p]$ (discretization of the boundary condition (24)) of the function with grid values $\mathbf{V}^n$, with different number of nodes each case, this fact is indicated by the vector so it does not cause confusion. In this case $\boldsymbol{\Pi}_j = \Pi(a_j)$, $\boldsymbol{\delta}_j^{n+1} = \delta(a_j, O^{n+1})$, $\boldsymbol{\delta}_j^{n+1,*} = \delta(a_j, O^{n+1,*})$, $\boldsymbol{\sigma}_j^{n+1} = \sigma(a_j, G^{n+1})$, $0 \leq j \leq J_p$, and $\boldsymbol{\delta}^{n+1} \cdot \boldsymbol{\Pi} \cdot \mathbf{Q}^{n+1}$, $\boldsymbol{\delta}^{n+1,*} \cdot \boldsymbol{\Pi} \cdot \mathbf{Q}^{n+1,*}$, $\boldsymbol{\sigma}^{n+1} \cdot \boldsymbol{\Pi} \cdot \mathbf{Q}^{n+1}$, denote the componentwise product of the involved vectors. Here, a second order quadrature rule is appropriate, and we propose the composite trapezoidal quadrature rule. We point out that our method is completely explicit and also shows a good behaviour in the long-time integration to get the approximations to the theoretical steady state. We do not describe its convergence analysis because it is beyond the purposes of this work.

5. Numerical Experiments

We present in this section the analysis performed to experimentally check the behavior of the proposed numerical method with different test problems. The first test consists in confronting predictions of the theoretical analysis (steady state values) with the method's ability to generate a good approximation to the solution of the problem, even in the case of a long time integration allowing to approach steady state values. The second test aims at showing the capacity to obtain an accurate approximation when confronting the model to real biological data: we simulate an experimentally-induced anemia in mice and the response of the organism. The accuracy in the numerical integration is more important in this case than the long time integration.

In order to perform each test, we have used the functions α, σ and δ defined in (1)-(3).

The average lifespan of an erythrocyte is known to be 40 days in mice [21], so we assume a constant mortality rate, $\gamma(a,t) = \gamma = 1/40 \text{ d}^{-1}$.

Finally, the following Hill functions have been used in (6),

$$f(E) = C_f \frac{\theta_f^{n_f}}{\theta_f^{n_f} + E^{n_f}}, \qquad g(E) = C_g \frac{\theta_g^{n_g}}{\theta_g^{n_g} + E^{n_g}}, \tag{26}$$

where (avoiding the subscripts) $C > 0$ denotes the maximum of the function, $\theta > 0$ a threshold value, and $n > 1$ a sensitivity parameter.

Parameter values are listed in Tables 1 and 3. Some values have been obtained from existing values in the literature, others have been estimated using a classical minimization of a weighted residual sum of squares in order to fit biological measurements (this is indicated by [NS] in Tables 1 and 3).

Test Problem 1. The following numerical experiment shows the efficacy of the numerical method in simulating our model. To this end, we compare the behavior of the numerical solution with the solution provided by the theoretical analysis in section 3. In this section, existence of a unique positive stationary population density was shown, and we shall use it in the comparison of the numerical order of convergence of our scheme. We will show the optimal rate of convergence obtained with the numerical method.

We take the functions in (1)-(3) and (26) and use the parameter values in Table 1.

In order to avoid discontinuities caused by an incompatible initial condition, we use

$$s_0(a) = \frac{1}{7}\tau_p \, HSC \, \sigma(0, GC_0) \, (1 - a/\tau_c), \quad a \le \tau_c,$$

$$e_0(a) = \begin{cases} A \, HSC \left(\dfrac{C_{\delta_1}}{5} + \dfrac{\delta_2(0, Epo_0)}{6} \right) (\tau_p - a), & a \le \tau_p, \\ 0, & a > \tau_p, \end{cases}$$

and for $a \le \tau_p$,

$$\begin{aligned} p_0(a) &= HSC \left(1 - \frac{a}{\tau_p}\right)^5, \\ q_0(a) &= \frac{p(a,0)}{\Pi(a)}, \end{aligned} \tag{27}$$

Table 1: **Parameter values**. Sources of parameter values are given between brackets, with [NS] = values obtained by performing numerical simulations. The values of θ_α, θ_σ, C_f and C_g are respectively given by $\theta_\alpha^* = \log_{10}(2Epo^*)$, $\theta_\sigma^* = \log_{10}(3GC^*)$, $C_f^* = k_{epo}Epo^*(\theta_f^{n_f} + (E^*)^{n_f})/\theta_f^{n_f}$, $C_g^* = k_{gc}GC^*(\theta_g^{n_g} + (E^*)^{n_g})/\theta_g^{n_g}$. (N.U. = no unit)

Par.	Value	Unit	Par.	Value	Unit
Cell Populations [21], [NS]			Growth factors [20]		
A	2^8	N.U.	k_{Epo}	5.55	day^{-1}
HSC	10^4	$\text{cells.g}^{-1}\text{.d}^{-1}$	Epo^*	5.7	$\text{mU.}\mu\text{L}^{-1}$
γ	1/40	d^{-1}	k_{GC}	11.1	d^{-1}
E^*	1.51×10^7	cells	GC^*	44.6	$\text{mU.}\mu\text{L}^{-1}$
Cell Cycle and Differentiation Durations [21]					
τ_p	4	d	τ_c	1	d
Apoptosis Rate [21], [NS]			Self-Renewal Rate [21], [NS]		
C_α	0.6	d^{-1}	C_σ	1	d^{-2}
θ_α	θ_α^*	$\text{mU.}\mu\text{L}^{-1}$	θ_σ	θ_σ^*	$\text{mU.}\mu\text{L}^{-1}$
n_α	2	N.U.	n_σ	2	N.U.
Differentiation Rate [21], [NS]					
C_{δ_1}	1.15	d^{-1}	θ_δ	1	$\text{mU.}\mu\text{L}^{-1}$
C_{δ_2}	0.1	d^{-1}	n_δ	2	N.U.
Epo Production Rate [20], [NS]			GC Production Rate [20], [NS]		
C_f	C_f^*	$\text{mU.}\mu\text{L}^{-1}\text{.d}^{-1}$	C_g	C_g^*	$\text{mU.}\mu\text{L}^{-1}\text{.d}^{-1}$
θ_f	$0.7E^*$	cells.g^{-1}	θ_g	$0.4E^*$	cells.g^{-1}
n_f	7	N.U.	n_g	6	N.U.

which satisfy the first compatibility condition. Note that (27) is well defined. We complete the initial condition with $Epo_0 = 5$ $\text{mU.}\mu\text{L}^{-1}$ and $GC_0 = 44$ $\text{mU.}\mu\text{L}^{-1}$.

We do not know the analytical solution to the problem then, in order to compare with the numerical solution, we use the value of the steady state of the problem, given by the following formulae

$$s^*(a) = HSC\,\frac{\sigma(0,GC^*)\,i_1}{1-2\,\sigma(0,GC^*)\,i_1\,e^{-\alpha(a,Epo^*)\,\tau_c}}\,e^{-\alpha(a,Epo^*)\,a}, \quad a \le \tau_c, \tag{28}$$

$$e^*(a) = A\,HSC\,\frac{C_{\delta_1}i_{-1} + \delta_2(0,Epo^*)\,i_0}{1-2\,\sigma(0,GC^*)\,i_1\,e^{-\alpha(a,Epo^*)\,\tau_c}}\,e^{-\gamma\,a}, \quad a \le \tau_p, \tag{29}$$

$$p^*(a) = HSC\,\frac{e^{-a\,(\alpha(a,Epo^*)+\delta_2(a,Epo^*)+(1-a/(2\,\tau_p))\,\sigma(0,GC^*))}}{1-2\,\sigma(0,GC^*)\,i_1\,e^{-\alpha(a,Epo^*)\,\tau_c}}\,\left(1-\frac{a}{\tau_p}\right)^{\tau_p\,C_{\delta_1}}, \quad a \le \tau_p, \tag{30}$$

$$q^*(a) = HSC\,\frac{e^{-a\,(\alpha(a,Epo^*)+\delta_2(a,Epo^*)+(1-a/(2\,\tau_p))\,\sigma(0,GC^*))}}{1-2\,\sigma(0,GC^*)\,i_1\,e^{-\alpha(a,Epo^*)\,\tau_c}}, \quad a \le \tau_p, \tag{31}$$

where, for $r = -1, 0, 1$,

$$i_r = \int_0^{\tau_p}\left(1-\frac{a}{\tau_p}\right)^{C_{\delta_1}\tau_p+r}\,e^{-[\alpha(a,Epo^*)+\delta_2(a,Epo^*)+(1-a/(2\,\tau_p)\sigma(0,GC^*)]a}da.$$

h	$\mathcal{E}_h^p$	$\mathcal{E}_h^s$	$\mathcal{E}_h^e$	$\mathcal{E}_h^{Epo}$	$\mathcal{E}_h^{GC}$
3.125e-2	5.6446e-3	3.4988e-3	5.1756e-1	2.3044e-6	1.6660e-5
1.5625e-2	1.4187e-3	8.8050e-4	1.3073e-1	5.7095e-7	4.1277e-6
	1.99	1.99	1.99	2.01	2.01
7.8125e-3	3.5520e-4	2.2052e-4	3.2773e-2	1.4241e-7	1.0296e-6
	2.00	2.00	2.00	2.00	2.00
3.9063e-3	8.8846e-5	5.5164e-5	8.2001e-3	3.5589e-8	2.5729e-7
	2.00	2.00	2.00	2.00	2.00
1.9531e-3	2.2236e-5	1.3806e-5	2.0524e-3	8.9049e-9	6.4378e-8
	2.00	2.00	2.00	2.00	2.00

Table 2: **Test problem 1.** Error and numerical convergence order, for $T = 1600$.

We have carried out an extensive numerical experimentation with different final-times T, step-sizes h and maximum erythrocites age $A_{\max}$ values. We observe that $A_{\max} = 1600$ is enough to obtain a good approximation to the non-truncated problem and $T = 1600$ produces a sufficiently long time integration in order to provide a numerical approximation to the steady state.

In Table 2, we present the results obtained with the method for different values of the step size. For each h, we compare at the final time $T = 1600$, the computed numerical solution $\mathbf{U}_h^n$, with the steady state $\mathbf{u}_h^n$, where $\mathbf{U}_h^n$ and $\mathbf{u}_h^n$ represent, respectively, $\mathbf{P}_h^n$, $\mathbf{S}_h^n$, $\mathbf{I}_h^n$, O^n and G^n and $\mathbf{p}_h^n$, $\mathbf{s}_h^n$, $\mathbf{e}_h^n$, Epo^* and GC^*, $0 \leq n \leq N$. In each row of Table 2, the upper number shows the maximum error with different step sizes h (first column); that is

$$\mathcal{E}_h^u = \max_{0 \leq n \leq N} \|\mathbf{U}_h^n - \mathbf{u}^n\|_\infty,$$

and the lower number the numerical order of convergence, which we compute with the formula

$$s_{2\,h}^u = \frac{\log(\mathcal{E}_{2\,h}^u / \mathcal{E}_h^u)}{\log(2)}.$$

Results in Table 2 clearly confirm the expected second-order of convergence.

Test Problem 2. The second test deals with the reproduction of biological measurements. Data come from an experiment of induced anemia in mice, introduced in [21]. We assume that the initial condition of the system is given by the steady state (28)-(31), then we simulate the anemia (induced by a drug called phenylhydrazine that kills red blood cells upon injection on days 0 and 1, see Figure 2) and we observe the reaction of the organism that leads to full recovery within few days (see Figure 2). Thus, we are not interested on a long time integration but rather on an accurate description of transient dynamics.

Let first recall that "hematocrit" is a test that measures the volume of red blood cells in a blood sample. It gives a percentage of erythrocyte volume found in the whole blood volume. It can be considered [21] that a blood sample is mainly composed with erythrocytes and plasma, since platelet and white cell volumes can be easily neglected. The system (4)-(6) is then numerically solved with the method proposed in section 4, and the corresponding simulated

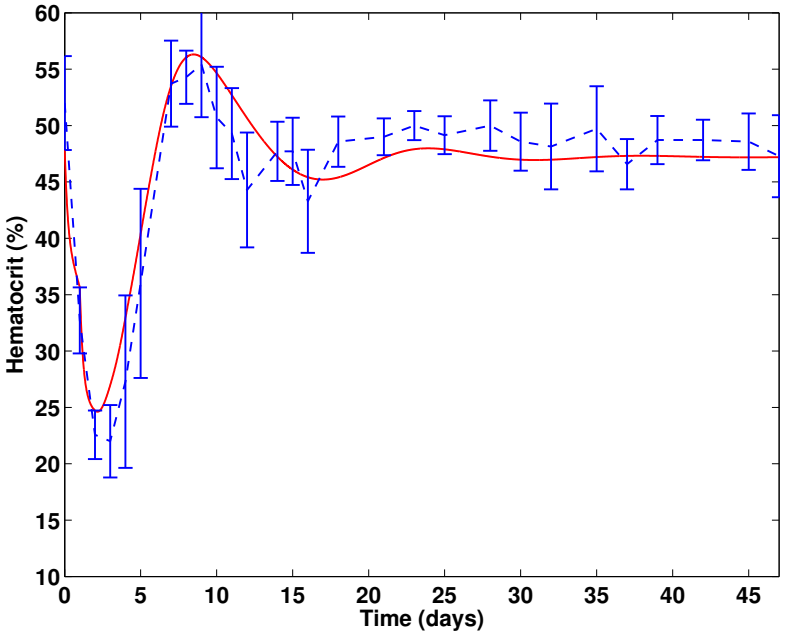

Figure 2: **Experimental and Simulated Hematocrits.** Experimental data are given by the blue dashed line, with error bars on every experimental time point. The simulated hematocrit is given by the red curve. Mice are rendered anemic by two consecutive injections of phenylhydrazine on days 0 and 1. The hematocrit shows a strong fall following the anemia (the hematocrit reaches very low values), then it rapidly increases to reach a high value, and then returns to the equilibrium. The simulated hematocrit is able to correctly capture all these features. All parameter values are given by Tables 1 and 3.

hematocrit HCT is computed using the formula in [21],

$$HCT(t) = \frac{E(t)}{E(t) + E^*(1 - HCT^*)/HCT^*},$$

where $E(t)$ is the total number of erythrocytes and HCT^* is the steady state value of the hematocrit, obtained through experimental data (in mice, HCT^* is around $45\% - 50\%$, see Figure 2).

Again, we use the functions in (1)-(3) and (26) to perform the simulations. We have carried out an extensive numerical experimentation with different final-times T, step-sizes h and values of the parameters involved in the problem. We observe that $T = 200$ and $h = 7.8125\text{e}{-3}$ provide sufficiently accurate approximations to the theoretical stationary state.

In [21] the authors noticed that in order to correctly reproduce experimental data (the rapid increase of the hematocrit following anemia and the damped oscillations observed after the peak of the response), a modification of the value of the mortality rate of erythrocytes should be accounted for. This has been identified as a consequence of using phenylhydrazine to induce anemia: one effect of this substance is to dramatically alter the lifespan of erythrocytes that were not killed by it (see [34] for a study on chicken's erythrocytes lifespan, as well as [17, 28, 29, 35]). We then introduce a modification of the erythrocyte

Table 3: **Parameter values**. Sources of parameter values are given between brackets, with [NS] = values obtained by performing numerical simulations. (N.U. = no unit)

Par.	Value	Unit	Par.	Value	Unit
Steady States [21], [NS]					
E^*	1.72×10^7	cells	HCT^*	48%	N.U.
Phenylhydrazine Injections [NS]					
R	2	d^{-1}	K	9	d^{-1}
t_f	1	d	m	4	N.U.
t_2	1	d			

mortality rate $\gamma(a,t)$, as follows

$$\gamma(t,a) = \gamma\ (1 + phz(a,t,0,t_f) + phz(a,t,t_2,t_f))\,,$$

where the function phz accounts for the effect of phenylhydrazine, as follows

$$phz(a,t,t_i,t_f)=\begin{cases} 0, & t \le t_i \text{ or } a \le t - t_i, \\ K\dfrac{(t_i + t_f - t)^m}{t_f^m} + R, & t_i \le t \le t_i + t_f \text{ and } a \ge t - t_i, \\ R, & t_i + t_f \le t \text{ and } a \ge t - t_i, \end{cases}$$

with t_i the time of the injection, t_f the duration of the phenylhydrazine effect in the blood, R a nonnegative residual effect, K a positive constant which determines the maximum effect of the phenylhydrazine injection, and m an exponent associated with the clearance of the phenylhydrazine while in blood.

In order to compare the model simulations with the experimental data, we then reproduced the experimental protocol consisting in two injections of phenylhydrazine, with the initial injection occurring at time $t = 0$ and the second injection at time $t_2 = 1$ day. Since experimentally both injections are similar (same dose, same route of injection), we assumed that they both have the same effects and we used the same parameter values for the function phz, except for the value of t_i. Additional parameter values are shown in Table 3.

Figure 2 shows the simulation performed numerically with $\gamma = 1/\sqrt{40}$, parameter data in Tables 1, and 3, and associated experimental data. One can appreciate how the numerical solution reproduces the behavior of the phenylhydrazine action in inducing anemia and the recovery of the organism.

6. Conclusions

We considered an age-structured partial differential equation system, coupled to a system of ordinary differential equations, which generalizes a previous model published in [21] to describe erythropoiesis. In addition to cell population dynamics, this new model incorporates growth factor dynamics, and explicitly considers an age-dependency of feedback control functions describing immature cell self-renewal and differentiation. The complexity of the mathematical model we considered limited the theoretical analysis that could be performed, however a study about the existence of steady states has been performed.

In order to perform a more complex analysis of the model, we needed to introduce numerical approximation to the solution. Therefore, we presented an "ad hoc" new numerical method to generate a simulated solution of the system.

We have studied numerically both its accuracy and its potential to simulate real biological behaviors, based on experimental data. On one hand, we have shown numerically a second order of convergence. On the other hand, the method proved able to accurately replicate an experimental protocol, consisting in injecting mice with a substance that kills red blood cells and induces anemia, which has been modeled following [8]. Thus, the numerical scheme shows a second order convergence in a finite time integration, a good behavior in a long-time one and it is able to simulate and replicate biological data.

Aknowledgements

FC work has been supported by ANR grant ProCell ANR-09-JCJC-0100-01. OA and JCLM have been supported in part by project MTM2014-56022-C2-2-P of the Spanish Ministerio de Economía y Competitividad and European FEDER Funds, and by Consejería de Educación, JCyL, project VA191U13.

[1] L. M. Abia, O. Angulo, J.C. López-Marcos. Age-structured population models and their numerical solution, Ecol. Model. 188 (2005) 112-136.

[2] A.S. Ackleh, K. Deng, K. Ito, J. Thibodeaux, A structured erythropoiesis model with nonlinear cell maturation velocity and hormone decay rate, Math. Bios. 204 (2006) 21–48, doi:10.1016/j.mbs.2006.08.004.

[3] A.S. Ackleh, J. Thibodeaux, Parameter Estimation in a Structured Erythropoiesis Model. Math. Bios. Eng. 5 (2008) 601-616.

[4] M. Adimy, F. Crauste, L. Pujo-Menjouet, On the stability of a maturity structured model of cellular proliferation, Discret. Cont. Dyn. Sys. Ser. A 12 (3) (2005) 501-522.

[5] M. Adimy, F. Crauste, S. Ruan, A mathematical study of the hematopoiesis process with applications to chronic myelogenous leukemia, SIAM J. Appl. Math. 65 (4) (2005) 328–1352.

[6] M. Adimy, F. Crauste, S. Ruan, Modelling hematopoiesis mediated by growth factors with applications to periodic hematological diseases. Bull. Math. Biol. 68 (8) (2006) 2321–2351.

[7] M. Adimy, O. Angulo, F. Crauste, J.C. López-Marcos, Numerical integration of a mathematical model of hematopoietic stem cell dynamics, Comput. Math. Appl., 56 (2008) 594–606.

[8] O. Angulo, F. Crauste, Investigating the Roles of the Experimental Protocol in Phenylhidrazine-Induced Anemia in Mice, J. Theor. Biol., submitted.

[9] O. Angulo, J.C. López-Marcos, M.A. Bees, Mass Structured Systems with Boundary Delay: Oscillations and the Effect of Selective Predation, J. Nonlinear Sci. 22 (2012) 961–984.

[10] O. Angulo, J.C. López-Marcos, M.A. López-Marcos, A numerical integrator for a model with a discontinuous sink term: the dynamics of the sexual phase of monogonont rotifera, Nonlinear Analysis: RWA 6 (2005) 935–954.

[11] O. Angulo, J.C. López-Marcos, M.A. López-Marcos, Numerical approximation of singular asymptotic states for a size-structured population model with a dynamical resource, Math. Comput. Model. 54 (2011) 1693–1698.

[12] O. Angulo, J.C. López-Marcos, M.A. López-Marcos, A semi-Lagrangian method for a cell population model in a dynamical environment Math. Comput. Model. 57 (2013) 1860–1866.

[13] O. Angulo, J.C. López-Marcos, M.A. López-Marcos, J. Martínez-Rodríguez, Numerical analysis of a population model of marine invertebrates with different life stages, Commun. Nonlinear Sci. Numer. Simul. 18 (2013) 2153–2163.

[14] O. Angulo, J.C. López-Marcos, M.A. López-Marcos, F.A. Milner, A numerical method for nonlinear age-structured population models with finite maximum age, J. Math. Anal. Appl. 361 (2010) 150–160.

[15] A. Bauer, F. Tronche, O. Wessely, C. Kellendonk, H.M. Reichardt, P. Steinlein, G. Schutz, H. Beug, The glucocorticoid receptor is required for stress erythropoiesis, Genes Dev. 13 (1999) 2996–3002.

[16] J. Bélair, M.C. Mackey, J.M. Mahaffy, Age-structured and two-delay models for erythropoiesis, Math. Biosci. 128 (1995) 317–346, doi:10.1016/0025-5564(94)00078-E.

[17] N.I. Berlin, C. Lotz, Life span of the red blood cell of the rat following acute hemorrhage, Proc. Soc. Exp. Biol. Med. 78 (1951) 788.

[18] C. Colijn, M.C. Mackey, A mathematical model of hematopoiesis – I. Periodic chronic myelogenous leukemia, J. Theor. Biol. 237 (2005) 117–132, doi:10.1016/j.jtbi.2005.03.033.

[19] C. Colijn, M.C. Mackey, A mathematical model of hematopoiesis – II. Cyclical neutropenia, J. Theor. Biol. 237 (2005) 133–146, doi:10.1016/j.jtbi.2005.03.034.

[20] F. Crauste, I. Demin, O. Gandrillon, V. Volpert, Mathematical study of feedback control roles and relevance in stress erythropoiesis, J. Theor. Biol. 263 (3) (2010) 303-316.

[21] F. Crauste, L. Pujo-Menjouet, S. Génieys, C. Molina, O. Gandrillon, Adding self-renewal in committed erythroid progenitors improves the biological relevance of a mathematical model of erythropoiesis, J. Theor. Biol. 250 (2008) 322–338.

[22] O. Gandrillon, U. Schmidt, H. Beug, J. Samarut, TGF-beta cooperates with TGF-alpha to induce the self-renewal of normal erythrocytic progenitors: evidence for an autocrine mechanism, Embo. J. 18 (1999) 2764–2781.

[23] S.M. Hattangadi, K.A. Burke, H.F. Lodish, Homeodomain-interacting protein kinase 2 plays an important role in normal terminal erythroid differentiation, Blood 115 (23) (2010) 4853-4861.

[24] M.J. Koury, M.C. Bondurant, Erythropoietin retards DNA breakdown and prevents programmed death in erythroid progenitor cells, Science 248 (1990) 378–381.

[25] M. Loeffler, K. Pantel, H. Wulff, H.E. Wichmann, A mathematical model of erythropoiesis in mice and rats. Part 1. Structure of the model, Cell Tissue Kinet. 22 (1989) 3–30.

[26] M.C. Mackey, Unified hypothesis of the origin of aplastic anaemia and periodic hematopoïesis, Blood 51 (1978) 941–956.

[27] J.M. Mahaffy, J. Belair, M.C. Mackey, Hematopoietic model with moving boundary condition and state dependent delay: applications in erythropoiesis, J. Theor. Biol. 190 (1998) 135–146, doi:10.1006/jtbi.1997.0537.

[28] K. Nagai, K. Oue, H. Kawagoe, Studies on the short-lived reticulocytes by use of the in vitro labeling method, Acta Haematol. Jpn 31 (1968) 967.

[29] K. Nagai, K. Ishizu, E. Kakishita, Studies on the erythroblast dynamics based on the production of fetal hemoglobin, Acta Haematol. Jpn 34 (1971).

[30] M. Iannelli, F.A. Milner, On the approximation of the Lotka-McKendrick equation with finite life-span, J. Comput. Appl. Math. 136 (2001) 245-254.

[31] L. Pujo-Menjouet, S. Bernard, M.C. Mackey, Long period oscillations in a G_0 model of hematopoietic stem cells, SIAM J. Appl. Dynam. Syst. 4 (2) (2005) 312–332.

[32] I. Roeder, Quantitative stem cell biology: computational studies in the hematopoietic system, Curr. Opin. Hematol. 13 (2006) 222–228.

[33] I. Roeder, M, Loeffler, A novel dynamic model of hematopoietic stem cell organization based on the concept of within-tissue plasticity, Exp. Hematol. 30 (2002) 853–861.

[34] A. Shimada, The maturation of reticulocytes. II. Life-span of red cells originating from stress reticulocytes, Acta Med. Okayama 29 (4) (1975) 283–289.

[35] F. Stohlman, Humoral regulation of erythropoiesis. VII. Shortened survival of erythrocytes by erythropoietin or severe anemia, Proc. Soc. Exp. Biol. Med. 107 (1961) 884.

[36] G. Webb, Theory of nonlinear age-dependent population dynamics, Monographs and textbooks in Pure and Appl. Math., vol 89, Marcel Dekker, New York, 1985.

[37] H.E. Wichman, M. Loeffler, Mathematical Modeling of Cell Proliferation, CRC, Boca Raton, FL, 1985.